GPS Solut (2011) 15:29–38
DOI 10.1007/s10291-010-0165-9

ORIGINAL ARTICLE

Variable length LMS adaptive filter for carrier phase multipath mitigation

Huicui Liu · Xiaojing Li · Linlin Ge · Chris Rizos · Feixue Wang

Received: 9 February 2009 / Accepted: 8 March 2010 / Published online: 1 April 2010

Abstract Multipath on carrier phase measurements is among the major error sources for short baseline positioning. A new method is proposed to improve the accuracy of the positioning results by mitigating the multipath effects on carrier phase measurements using the variable length Least Mean Square (VLLMS) adaptive filter. The performance of the filter is analyzed as well as compared with that of the standard LMS adaptive filter using a set of carrier phase observation data of two consecutive days collected in a short baseline experiment. Because the two antennas are static, the multipath error is the only dominant component in the carrier phase double-differenced residuals and indicates a repeated pattern. The numerical results show that both filters can significantly mitigate the multipath effects in carrier phase double-differenced residuals, and hence improve the positioning results. Furthermore, the VLLMS filter that reduces up to about 47.4% of the multipath effects on 3D positioning performs better than the LMS filter that only reduces 22.0%. Both filters are suitable for real-time applications.

Keywords GPS · Multipath · Carrier phase · LMS · Adaptive filter

H. Liu (✉) · F. Wang
School of Electronic Science and Engineering,
National University of Defense Technology,
410073 Changsha, China
e-mail: liuhuicui@nudt.edu.cn

X. Li · L. Ge · C. Rizos
School of Surveying and Spatial Information Systems,
University of New South Wales, Sydney 2052, Australia

Introduction

The multipath effect on GPS carrier phase measurements is small compared to multipath error in pseudorange measurements. In Kaplan and Hegarty (2006, p 290), the maximum carrier phase range error due to a single multipath is stated as being less than or equal to $\lambda/4$. This maximum is obtained when the multipath attenuation factor is less than or equal to unity. However, the multipath effect is still a major error source in the case of short baseline precise static positioning.

Multipath mitigation technologies or algorithms, for both pseudorange and carrier phase multipath, can be divided into three categories: antenna design, signal processing (or receiver design) and data processing. Through antenna design, such as the widely used choke ring antenna (Fillippov et al. 1998; Tranquilla et al. 1994), multipath signals from certain directions can be blocked, and the multipath effects on both pseudorange and carrier phase measurements are mitigated. However, such antennas cannot totally remove the multipath effect. Most signal-processing technologies, such as the Early Late Slope (ELS; Townsend and Fenton 1994) and Multipath Estimating Delay Lock Loop (MEDLL; Van Nee et al. 1994; Van Nee 1992; Townsend et al. 2000), behave well for the specular pseudorange multipath signals. Compared with the first two categories, data-processing techniques are the preferred way to address the multipath problem in carrier phase observations. Many data processing techniques, such as wavelet algorithms (Souza and Monico 2004) and signal-to-noise-based techniques (Comp and Axelrad 1996), have been suggested for multipath mitigation. The Least Mean Square (LMS) adaptive filter was first applied for GPS multipath mitigation by Ge et al. (2000). However, this LMS filter had both fixed tap numbers and a fixed step size.

In this paper, an enhanced LMS filter with variable length, known as a VLLMS adaptive filter (Bilcu et al. 2002), is used to mitigate multipath effects on carrier phase observations.

Multipath effects in double-differenced carrier phase observations

Multipath effects on carrier phase observations can be calibrated using double-differenced (DD) data. Figure 1 shows the geometric relationship of a single baseline, where m and n represent two ground antennas, while p and q represent two satellites. The carrier phase observation data of satellite $i(i = p, q)$ received by antenna $j(j = m, n)$ can be written as (Kaplan and Hegarty 2006, p 400–403):

$$\Phi_j^i = \rho_j^i + \varphi^i - \lambda N_j^i - c\left(\tau^i + \tau_j\right) + \mathrm{MP}_j^i + I_j^i - T_j^i + \sigma_j^i \qquad (1)$$

where Φ_j^i is the carrier phase variation measurements in meters between satellite $i(i = p, q)$ and antenna $j(j = m, n)$; ϕ^i is the carrier phase at the moment of transmission from satellite i; ρ_j^i is the geometric distance from satellite i to antenna j; N_j^i is the unknown integer number of carrier cycles; MP_j^i is the phase error due to the multipath; λ is the wavelength of the satellite signal and c is the propagation speed of light; τ^i and τ_j are the associated satellite and receiver clock bias, respectively; I_j^i and T_j^i are the advance of the carrier due to the ionosphere and the delay of the carrier due to the tropospheric, respectively; and σ_j^i is the phase error due to other sources.

The carrier phase DD data associated with the two satellites and the two receiver antennas can be written as:

$$\begin{aligned}\mathrm{DD} &= \left(\Phi_m^p - \Phi_m^q\right) - \left(\Phi_n^p - \Phi_n^q\right) \\ &= \Delta\nabla\rho_{mn}^{pq} + \lambda\Delta\nabla N_{mn}^{pq} + \Delta\nabla I_{mn}^{pq} + \Delta\nabla T_{mn}^{pq} \\ &\quad + \Delta\nabla\mathrm{MP}_{mn}^{pq} + \Delta\nabla\sigma \end{aligned} \qquad (2)$$

With the formation of the DD, the initial carrier phase, receiver and satellite clock biases are cancelled (Kaplan and Hegarty 2006, p 400–403). The remaining components are $\Delta\nabla\rho_{mn}^{pq}$ representing the linear combination of ρ_j^i, $\lambda\Delta\nabla N_{mn}^{pq}$ consisting of the combined unknown integer ambiguities, multipath effect combination $\Delta\nabla\mathrm{MP}_{mn}^{pq}$, a system phase noise term $\Delta\nabla\sigma$ attributable primarily to receiver effects (Walsh 1992), and $\Delta\nabla I_{mn}^{pq}$ and $\Delta\nabla T_{mn}^{pq}$ being the combined ionospheric and tropospheric effects, respectively. All terms are expressed in units of meters. In particular, $\Delta\nabla\mathrm{MP}_{mn}^{pq}$ can also be written in the form of differential multipath effects associated with the two satellites and the two receiver antennas, as in the following equation:

$$\Delta\nabla\mathrm{MP}_{mn}^{pq} = \left(\mathrm{MP}_m^p - \mathrm{MP}_m^q\right) - \left(\mathrm{MP}_n^p - \mathrm{MP}_n^q\right) \qquad (3)$$

In order to calibrate the multipath effects on the DD carrier phase data, the baseline between the two antennas should be comparatively short, typically less than 10 km (Weinbach et al. 2009), in order that the ionospheric and tropospheric effects can be assumed to largely cancel. For static antennas, ρ_j^i can be calculated using the known satellite coordinates (x^i, y^i, z^i) and the coordinates of the antenna (x^i, y^i, z^i) as follows:

$$\rho_j^i = \sqrt{\left(x^i - x_j\right)^2 + \left(y^i - y_j\right)^2 + \left(z^i - z_j\right)^2} \qquad (4)$$

Then $\Delta\nabla\rho_{mn}^{pq}$ can be computed and removed from the DD carrier phase data. The ambiguities N_j^i can be computed from:

$$N_j^i = \mathrm{floor}\left(\frac{\rho_j^i}{\lambda}\right)$$

where floor means rounding toward minus infinity. The term $\Delta\nabla N_{mn}^{pq}$ that is a linear combination of N_j^i can then be computed and removed. The multipath effect is now the dominant error component in the DD residuals, denoted by DD′, which can be written as:

$$\mathrm{DD}' = \Delta\nabla\mathrm{MP}_{mn}^{pq} + \Delta\nabla\sigma \qquad (5)$$

where the noise $\Delta\nabla\sigma$ is not correlated with $\Delta\nabla\mathrm{MP}_{mn}^{pq}$.

In the short baseline situations, the multipath effects on carrier phase measurements made to a certain satellite by a specific antenna can be analyzed if the following conditions are satisfied:

(a) One antenna (the "base antenna") should be located in an open sky view location, and therefore assumed to be in a relatively multipath-free area, while the other (the "rover antenna") is assumed to be multipath affected.
(b) During the observation period, a satellite with a high elevation is considered to be comparatively multipath free and serves as the "reference satellite".
(c) The two antennas are static.

With assumptions (a) and (b), and using Eq. (3), $\Delta\nabla\mathrm{MP}_{mn}^{pq}$ is equivalent to the multipath effects of the non-reference satellite at the rover receiver antenna. With assumption (c), the multipath effect on carrier phase at

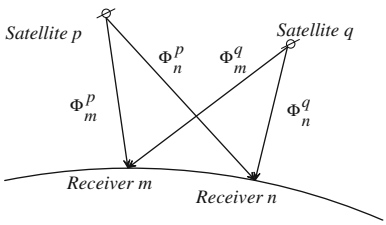

Fig. 1 Double-differenced GPS observations and their geometric relationship to a baseline

some epoch is correlated with the multipath effect at the same epoch of the next sidereal day. This is due to the fact that the azimuth and elevation of the GPS satellites and the receiver-reflectors' locations repeat every sidereal day (approximately 4 min shorter than a mean solar day). Therefore, multipath effects can be removed from carrier phase data by making use of the correlation characteristics (Ge et al. 2000). As a consequence, the positioning calculation based on the modified (multipath-mitigated) observation data can achieve higher accuracy.

The LMS adaptive filter

The general configuration of the LMS adaptive filter is shown in Fig. 2. The input signal can be represented as:

$$r(n) = x(n) + u(n) \tag{6}$$

where $x(n)$ is the desired signal and $u(n)$ is the noise distortion. The three signals have the same vector length N. Assume $d(n)$ is the reference signal, and also has the vector length N.

In order to extract the relatively noise-free signal from the input signal, the functions $x(n)$, $u(n)$ and $d(n)$ should fulfill the following conditions (Ge et al. 2000):

(a) The reference signal is correlated with the desired signal, such that:

$$E[d(n)x(n-k)] = p(k); \quad n,k = 0,\ldots N-1 \tag{7}$$

where $p(k)$ is an unknown cross-correlation for lag k.

(b) The noise is correlated with neither the reference signal nor the desired signal, such that:

$$E[x(n)u(n-k)] = 0; \quad n,k = 0,\ldots N-1 \tag{8}$$

$$E[d(n)u(n-k)] = 0; \quad n,k = 0,\ldots N-1 \tag{9}$$

By using the LMS filter that part of the input signal that is correlated with the reference signal can be extracted. As shown in Fig. 2, the functions $y(n)$ and $e(n)$ represent the output of the filter and the estimation error, respectively.

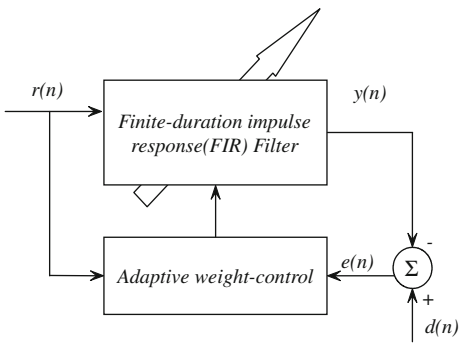

Fig. 2 LMS filter configuration

The output signal $y(n)$ is the part extracted from $r(n)$ that is correlated with $d(n)$. In the ideal situation $y(n) = x(n)$.

Based on the analysis in the second section, the zero-mean DD residuals in a short baseline experiment on a certain day, as indicated in Eq. (5), can be written in the form of Eq. (6), where $x(n)$ is the multipath sequence ΔMP and $u(n)$ is the uncorrelated noise ε. The multipath sequence for another day is then expressed as:

$$d(n) = x\prime(n) + u'(n) \tag{10}$$

where $x'(n)$ and $u'(n)$ have similar definitions as $x(n)$ and $u(n)$. The length of these four vectors is N.

Since the noise is uncorrelated with the multipath effects, and the noise signals of the 2 days are uncorrelated with each other, the signals $x(n)$, $x'(n)$, $u(n)$ and $u'(n)$ satisfy Eq. (7):

$$\begin{aligned} E[d(n)x(n-k)] &= E[(x'(n)+u'(n))x(n-k)] \\ &= E[x'(n)x(n-k)] = p(k); \\ & n,k = 0,\ldots N-1 \end{aligned} \tag{11}$$

$$E[x(n)u(n-k)] = 0; \quad n,k = 0,\ldots N-1 \tag{12}$$

$$\begin{aligned} E[d(n)u(n-k)] &= E[u'(n)u(n-k)] = 0; \\ & n,k = 0,\ldots N-1 \end{aligned} \tag{13}$$

In this way, the LMS filter can extract multipath effects (the correlated part) from DD residuals. Then, in the multipath mitigation background, $y(n)$ in Fig. 2 is the extracted multipath effects and $e(n)$ is the multipath-reduced DD residuals. Also, $y(n) = x(n)$ in the ideal situation, which means that all multipath effects in the input signal have been extracted.

In Fig. 2, the filter coefficients $h(n)$ with length M are controlled by an adaptive weight-control unit in which a LMS algorithm has been introduced. In a real-time implementation, $h(n)$ can be expressed as:

$$h_i(n+1) = h_i(n) + \mu e(n) r(n-i) \tag{14}$$

where μ is the step-size parameter, and $h_i(n)$ ($i = 0, 1,\ldots, M-1$) refers to the ith tap weight of the filter, $n = 0, 1,\ldots, N-1$. Hence, $y(n)$ and $e(n)$ can be expressed as:

$$y(n) = \sum_{i=0}^{M-1} h_i(n) r(n-i) \tag{15}$$

$$e(n) = d(n) - y(n). \tag{16}$$

The filter length M and the step-size parameter μ should be carefully chosen to ensure that the LMS algorithm converges rapidly and is stable. Ge et al. (2000) and Haykin (2002) discuss the selection of the appropriate filter length and step-size parameter.

In Haykin (2002, pp 66–67), the optimal filter length is discussed with respect to the minimum description length (MDL) criterion, which is defined as:

$$\mathrm{MDL}(M) = -L(\hat{\theta}_M) + \frac{1}{2} M \ln N \tag{17}$$

where $L(\hat{\theta}_M)$ is the logarithm of the maximum likelihood estimates of the filter parameters. The first term tends to decrease with increasing M, while the second term increases linearly with increasing M. Hence, the optimal M can balance the two trends in order to minimize MDL. In Ge et al. (2000), the filter length is selected as one for multipath data processing. As a result of some simulations using the data collected in the experiment mentioned above, the optimal filter length was found to be unity, and this value is used in this paper.

To ensure stability, the step-size parameter μ should be in the range (Ge et al. 2000):

$$0 < \mu < \frac{M+1}{10M \sum_{n=0}^{N-1} d^2(n)} \tag{18}$$

where M is the filter length.

The variable length LMS adaptive filter

The LMS filter can be easily applied, and hence it has become very popular. However, almost all implementations known to the authors use some fixed, predefined filter values. Although there are some implementations of variable length LMS (VLLMS) adaptive filters (Pritzker and Feuer 1991), their performance is not steady.

In Bilcu et al. (2002), a variable LMS adaptive filter was introduced whose configuration is illustrated in Fig. 3.

There are three parallel filters, with each of them being identical to those illustrated in Fig. 2. The coefficient vector of filter l is $h_i(n)$ with length M_l (l = 1, 2, 3); the functions $r(n)$ and $d(n)$ represent, respectively, the input signal and reference signal defined in the LMS filter section; and the functions $y_l(n)$ and $e_l(n)$ (l = 1, 2, 3) represent the output signal and estimation errors of filter l, respectively. The three estimation errors $e_l(n)$ (l = 1, 2, 3) are input into a length control unit that computes estimates of the mean

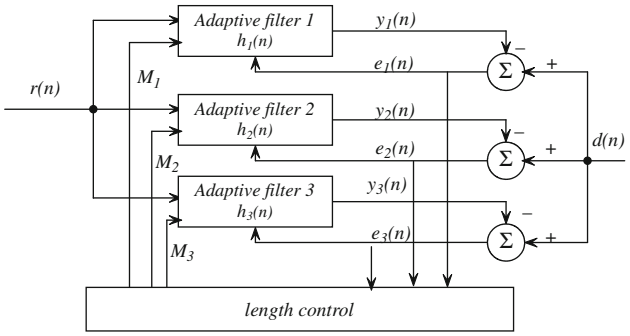

Fig. 3 VLLMS filter configuration after Bilcu et al. (2002)

square error (MSE) for each filter, and based on these estimates, the updated filter lengths are generated. The operation of the algorithm can be summarized as follows:

(1) Initialization:

$$M_1(0) = M_0,\ M_2(0) = M_0 + 1,\ M_3(0) = M_0 + 2 \tag{19}$$

$$h_1(0) = 0_{N_1},\ h_2(0) = 0_{N_2},\ h_3(0) = 0_{N_3} \tag{20}$$

$$\mu_1(0) = \frac{\mu M_0}{M_1(0)},\ \mu_2(0) = \frac{\mu M_0}{M_2(0)},\ \mu_3(0) = \frac{\mu M_0}{M_3(0)} \tag{21}$$

where M_0 and μ are the initial filter length and step-size parameter for filter one, respectively.

(2) For each k = 1, 2,…:

(a) Compute the output errors:

$$e_l(k) = d(k) - \sum_{i=0}^{M_l - 1} h_{li}(k) r(k-i+1); \quad l = 1, 2, 3 \tag{22}$$

where $h_{li}(k)$ is the ith tap weight of the adaptive filter l.

(b) Update the coefficients:

$$h_l(k+1) = h_l(k) + \mu_l(k) r_l(k) e_l(k); \quad l = 1, 2, 3 \tag{23}$$

(c) At each Lth iteration:

- Compute the following averages:

$$m_l = \frac{1}{L} \sum_{j=k-L+1}^{k} e_l^2(j); \quad l = 1, 2, 3 \tag{24}$$

- Update the lengths:

$$M_1(k+1) = \begin{cases} M_1(k) + 1, & \text{if } m_1 > m_2 > m_3 \\ M_1(k), & \text{if } \begin{cases} m_1 > m_2 \\ m_{22} \le m_{33} \end{cases} \\ M_1(k) - 1, & \text{otherwise} \end{cases} \tag{25}$$

$$\begin{aligned} M_2(k+1) &= M_1(k+1) + 1, M_3(k+1) \\ &= M_1(k+1) + 2 \end{aligned} \tag{26}$$

- Update the step sizes:

$$\mu_l(k+1) = \frac{\mu N_0}{M_l(K+1)}; \quad l = 1, 2, 3 \tag{27}$$

vwhere m_i (i = 1, 2, 3) acts as the statistic square error in this algorithm. It is shown in Bilcu et al. (2002) that for an uncorrelated input signal $r(n)$ that satisfies $E[r(n)r(n-k)] = 0$ for $k \neq 0$, the following is valid:

$$\frac{J_{\infty}^{(l)}}{J_{\infty}^{(m)}} = \frac{J_{\min}^{(l)}}{J_{\min}^{(m)}} = \begin{cases} \geq 1, & \text{if} \quad M_1 \leq M_2 < M_{\text{opt}} \\ < 1, & \text{if} \quad M_2 < M_1 < M_{\text{opt}} \\ 1, & \text{if} \quad M_1 > M_{\text{opt}} \text{ or } M_2 > M_{\text{opt}} \end{cases} ; \quad l = 1,2,3, \quad m = 1,2,3, \quad l \neq m \tag{28}$$

when the following relation holds at each iteration:

$$\mu_1(k)N_1(k) = \mu_2(k)N_2(k) = \mu_3(k)N_3(k) \tag{29}$$

where $J_{\infty}^{(l)} = E[e^2(\infty)^{(l)}]$, $l = 1,2,3$ is the steady-state MSE, and $J_{\min}^{(l)}$, $l = 1,2,3$ is the minimum steady-state MSE and M_{opt} is the optimal filter length. Hence, in this new algorithm, Eq. (25) guarantees the filter length has an optimal value. The second filter is the filter of interest in the sense that its coefficients vector will be the closest one to the Wiener filter.

Selecting an optimum L is very important for the algorithm. The number of iterations L should be small enough in order to update m_i ($i = 1, 2, 3$) quickly. However, the selected L should be large enough to have a sufficient number of updates. Unfortunately, there is still no theoretical optimum value for L, and hence in this paper, L is selected as one (based on simulation tests carried out using the collected data).

Note that Eq. (28) would not be valid if the input signal is correlated. However, for this application, it can be assumed that the multipath sequence for carrier phase is random, i.e., uncorrelated.

The short baseline experiment

A short baseline experiment was carried out in order to investigate the multipath effects on double-differenced carrier phase data. The experiment involved a baseline of approximately 200 m in length, observed over two successive days in Centennial Park, Sydney (Australia) (Fig. 4). The Base antenna was in an open (assumed comparatively) multipath-free playground area (the right photograph in Fig. 4), while the Rover antenna was located near the Federal Pavilion (the left photograph in Fig. 4). The experiments were carried out from about 10:00 am to 12:00 pm (GMT+10), on September 10 and 11, 2008, when satellite PRN18 reached its peak elevation at this location. Two Leica GX1230 GNSS receivers were used to collect carrier phase data. The Rover antenna type was the Leica AX1202, and the Base antenna was the Leica AT504, a choke ring antenna that can mitigate the multipath signals reflected by the ground.

Figure 5 shows the elevations of five visible satellites used in the experiment. There were also some other satellites visible at the same time; after tested by Leica software these five satellites are one of the satellites groups that can provide the position results. So in this paper, only these five were used for positioning for simplicity. Concerning these five satellites, PRN 18 is the only satellite during the experiment that reached its peak elevation.

The DD residuals associated with Rover and Base receivers are plotted in Fig. 6 (in metric units), with PRN18 as the reference satellite. The data of the first day were collected from 10:24:25 to 11:22:45 (GMT+10) sampled at 0.2 Hz, while the data of the second day were collected 4 min earlier. The correlation between the L1 DD residuals of the 2 days can be clearly seen, with the correlated part mainly due to multipath effects. The overall variation of the DD residuals of PRN22 is the smallest among the four non-reference satellites because its elevation was the highest during most of the experiment.

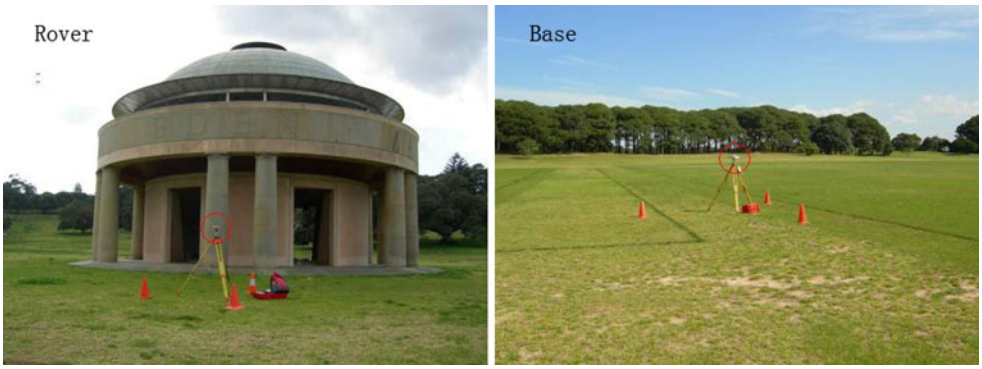

Fig. 4 The short baseline experiment environment

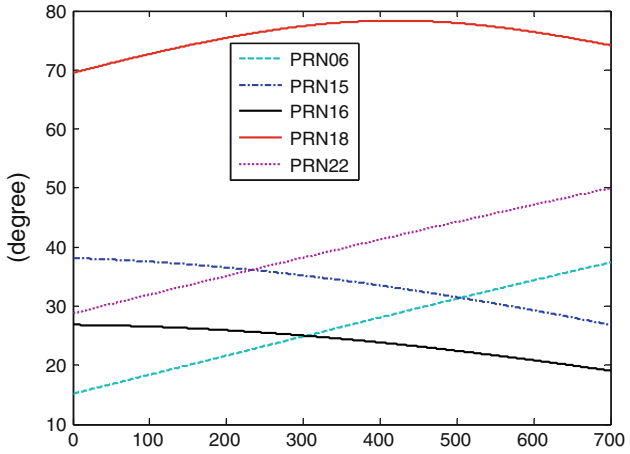

Fig. 5 Elevation angles of the satellites during the experiment

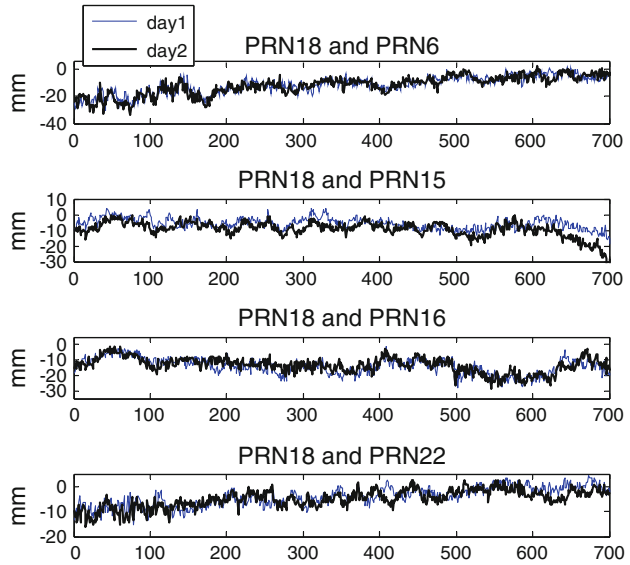

Fig. 6 L1 DD residuals time series

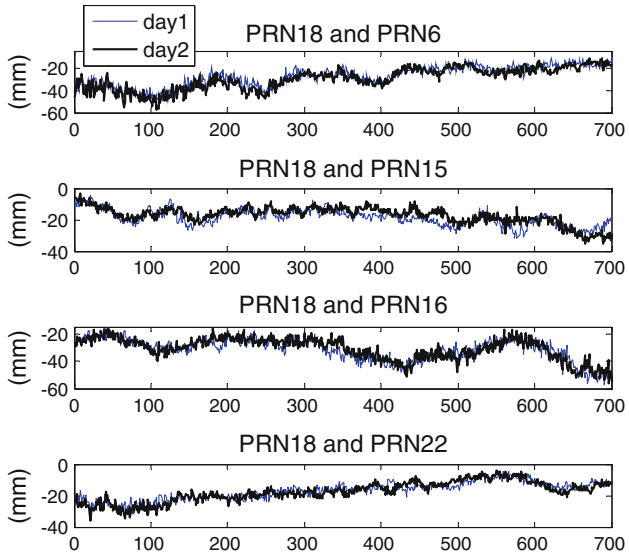

Fig. 7 L2 DD residuals time series

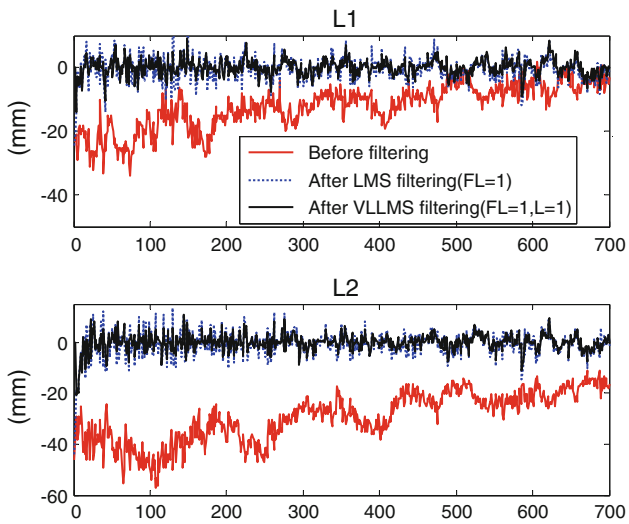

Fig. 8 DD residuals of PRN06 before and after filtering

Multipath mitigation and the positioning results

The L1 DD residuals are shown in Fig. 6, and the L2 data have similar characteristics as indicated in Fig. 7. The lowest elevation satellite introduces the largest multipath effects.

As discussed earlier, the correlated component between successive days' DD residuals can be extracted using either the LMS filter or the VLLMS filter. There are two different filtering processes: forward filtering and backward filtering. Forward filtering means that GPS results on a given day are used to correct results on the following day, while backward filtering has the inverse meaning (Ge et al. 2000). According to Liu et al. (2008), forward filtering is statistically better than backward filtering, and the larger the time difference between the reference and input signals, the less effective the multipath mitigation will be. In this paper, only forward filtering is used, and the reference signal and input signal are the DD residuals of two successive days. In other words, the DD residuals of the first day act as the reference signal, and the DD residuals of the second day are the input signal.

Figures 8 and 9 show the DD residuals for satellites PRN06 and PRN16 before and after filtering. The red line represents the input signals, which are the DD residuals of the first day (day1) before filtering. The blue dashed and

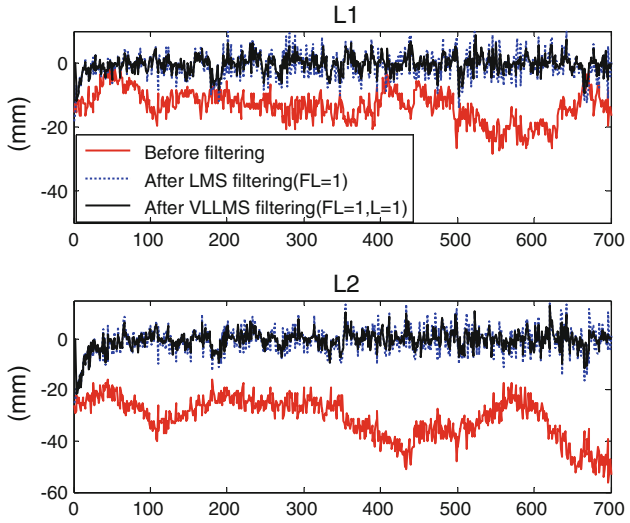

Fig. 9 DD residuals of PRN16 before and after filtering

Table 1 Mean of DD residuals of PRN06 (day2/day1, millimeters)

PRN06		Before multipath mitigation	After multipath mitigation	Improvement (%)
L1	LMS filtering	−12.3	−0.6	95.2
	VLLMS filtering		−0.1	99.9
L2	LMS filtering	−29.4	−0.6	97.8
	VLLMS filtering		−0.2	99.3

Table 2 Mean of DD residuals of PRN16 (day2/day1, millimeters)

PRN16		Before multipath mitigation	After multipath mitigation	Improvement (%)
L1	LMS filtering	−13.4	−0.8	93.7
	VLLMS filtering		−0.3	97.5
L2	LMS filtering	−30.6	−0.9	96.9
	VLLMS filtering		−0.6	98.0

Table 3 Standard deviation of DD residuals of PRN06 (day2/day1, millimeters)

PRN06		Before multipath mitigation	After multipath mitigation	Improvement (%)
L1	LMS filtering	6.9	3.4	50.9
	VLLMS filtering		2.5	64.0
L2	LMS filtering	9.7	4.2	56.9
	VLLMS filtering		3.1	68.6

Table 4 Standard deviation of DD residuals of PRN16 (day2/day1, millimeters)

PRN16		Before multipath mitigation	After multipath mitigation	Improvement (%)
L1	LMS filtering	4.9	3.6	27.3
	VLLMS filtering		2.9	40.5
L2	LMS filtering	8.0	4.4	44.8
	VLLMS filtering		3.5	57.1

the black lines represent the multipath-modified DD residuals of the two filters. In these two figures, the filtering length (FL) of the LMS filter, the initial filtering length (IFL) and the statistical length L of the VLLMS filter are all unity. From the statistical results in Tables 1, 2, 3, 4, one can see the mean of DD residuals after filtered converge at zero and the improvement in standard deviation of the DD residuals is up to 68.6%. Furthermore, the VLLMS performs better than the LMS filter.

Note that both the LMS filter and the VLLMS filter have a training time, which means that the two filters can converge to the tracking state only after a finite period of time. The length of the training time, which can be validated by using a impulse sequence as the input signal and depends on the initial coefficients of the filter initial coefficients, is about 60 samples for the adaptive filters used in this paper. Hence, the lengths of both the input signal and the reference signal should be long enough to ensure that there are sufficient output samples after the filter converges.

The performance of the two classes of filter can also be analyzed in the frequency domain. The correlation characteristics of the multipath effects on day1 and day2 can be more clearly seen from the FFT of their correlation vector. From Fig. 10, where the input signal $r(n)$ is the DD residual time series from day1 and the reference signal $d(n)$ represents the DD residual time series from day2, it can be concluded that $r(n)$ and $d(n)$ are strongly correlated since the FFT of R_{rd} is not "white":

$$R_{\mathrm{rd}}(k) = E[r(n)d(n-k)]; \quad n,k = 1,\ldots,N. \tag{30}$$

Figure 10 also shows the FFT of R_{ed} for the two filters, where:

$$R_{\mathrm{ed}}(k) = E[e(n)d(n-k)]; \quad n,k = 1,2\ldots,N. \tag{31}$$

and $e(n)$ is the estimation error of the filter, which should be uncorrelated with $d(n)$. According to the experimental results shown in Fig. 10, the frequency components of R_{rd} are mainly concentrated in the spectrum range 0–0.01 Hz. However, after filtering, the FFT of R_{ed} is obviously smoother, i.e., $e(n)$ is more like white noise. Also, the estimation error $e(n)$ of the VLLMS filter is "whiter" than

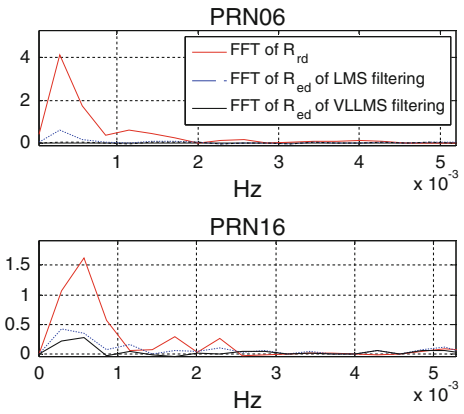

Fig. 10 The FFT of the correlation vector between input/output signal and reference signal before and after filtering (L1)

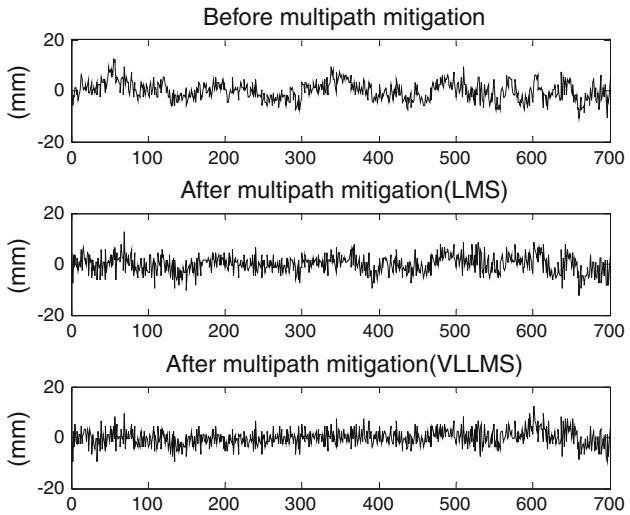

Fig. 11 Position results of *x*-coordinate component from forward filtering (day2/day1)

$e(n)$ of the LMS filter. As indicated by Eq. (11), the correlated components between $d(n)$ and $r(n)$ are the multipath effects.

Because the elevation of satellite PRN18 is much higher than satellites PRN06 and PRN16, the extracted multipath effects from the two sets of DD residuals can be considered to be the multipath effects on the carrier phase data of satellites PRN06 and PRN16. Also, the same assumption can be made for satellites PRN15 and PRN22. Then, after canceling the multipath effects from the carrier phase of the four lower elevation satellites, the more accurate position results based on the multipath-mitigated carrier phase data are shown in Figs. 11, 12, 13. Standard deviations of the three coordinate components and the 3D position results are presented in Table 5. It can be seen that the variability that

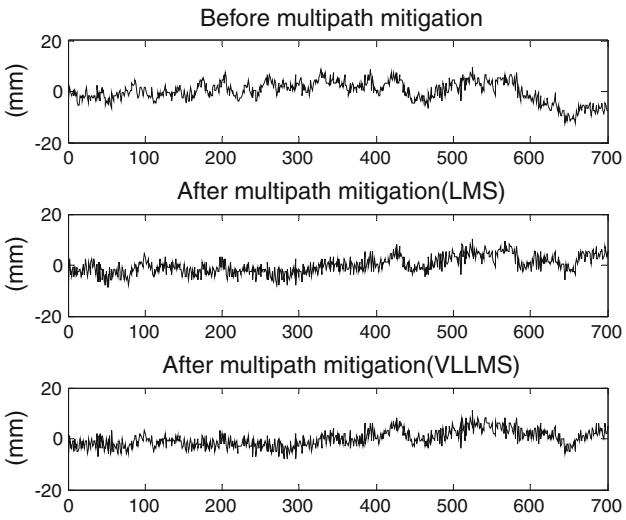

Fig. 12 Position results of *y*-coordinate component from forward filtering (day2/day1)

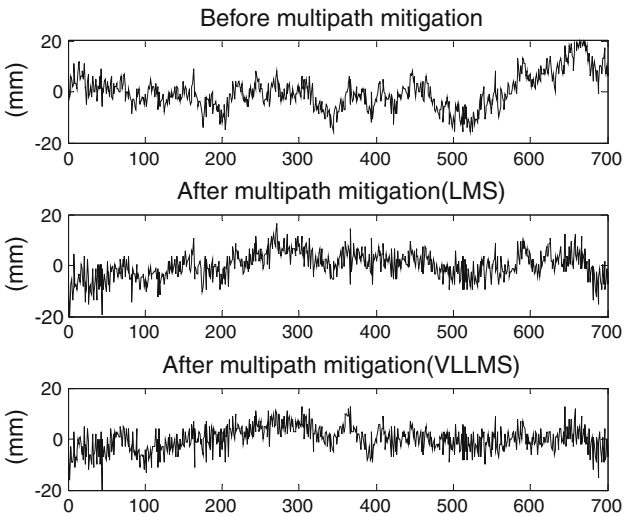

Fig. 13 Position results of *z*-coordinate component from forward filtering (day2/day1)

Table 5 Standard deviation of positioning results (day2/day1, millimeters)

Standard deviation		Before multipath mitigation	After multipath mitigation	Improvement (%)
X	LMS filtering	3.6	3.3	6.7
	VLLMS filtering		3.2	11.7
Y	LMS filtering	4.0	3.4	14.8
	VLLMS filtering		3.3	18.9
Z	LMS filtering	6.9	5.4	22.4
	VLLMS filtering		4.9	29.1
3-D	LMS filtering	5.4	4.2	22.0
	VLLMS filtering		2.8	47.4

existed before multipath mitigation has been suppressed, especially in the z-coordinate component. The improvement using the VLLMS filter is greater than using the LMS filter. About 47.4% of the multipath effect on 3D positioning can be reduced by using the VLLMS filter, while in the case of the LMS filter, this reduction is about 22.0%.

Concluding remarks

The authors have introduced a multipath mitigation method based on the VLLMS adaptive filter, and demonstrated it in a short baseline experiment. Compared with the widely used standard LMS adaptive filter, the VLLMS filter can provide better performance though there is a slight sacrifice in terms of additional computational complexity. Since the VLLMS filter comprises three parallel LMS filters, expect for the slight difference in the control unit, the two kinds of filters have the similar computational requirements. The algorithms have been tested on a baseline with one antenna at a comparatively multipath-free site and one satellite with high elevation angle (likely to have low multipath effect). Experimental results show that up to about 47.4% of the multipath effects on 3D positioning can be reduced using the VLLMS filter, while it is only 22.0% in the case of using the LMS filter. This algorithm has been tested using double-differenced carrier phase data from other satellite pairs in the same experiment and similar conclusions can be drawn.

Further, a software platform can be established by which the multipath effects on positioning results can be removed. After the training time, the time delay of filtering processing is small and if the data transmission from the two receivers to the software platform is real time, this algorithm can be used in real-time applications.

Acknowledgments The first author's overseas study is supported by the China Scholarship Council. The experiment described in the paper was carried out with the help of Mr. Cemal Ozer Yigit.

References

Bilcu RC, Kuosmanen P, Eguazarian K (2002) A variable length LMS algorithm: theoretical analysis and implementations. In: 9th International Conference on Electronics, Circuits and Systems, vol 3. pp 1031–1034

Comp CJ, Axelrad P (1996) An adaptive SNR-based carrier phase multipath mitigation technique. In: 9th International Technical Meeting of the Satellite Division of the U.S. Institute of Navigation. Kansas City, 17–20 Sep, pp 683–697

Fillippov V, Tatarnicov D, Ashjaee J, Astakhov A, Sutiagin I (1998) The first dual-depth dual-frequency choke ring. In: 11th International Technical Meeting of Satellite Division of the U.S. Institute of Navigation. Nashville, 15–18 Sep, pp 1035–1040

Ge L, Han SW, Rizos C (2000) Multipath mitigation of continuous GPS measurements using an adaptive filter. GPS Solut 4(2):19–30

Haykin SS (2002) Adaptive filter theory, 4th edn. Prentice-Hall, Upper Saddle River

Kaplan ED, Hegarty CJ (2006) Understanding GPS: principles and applications, 2nd edn. Artech House, London

Liu H, Li X, Ge L, Rizos C, Wang F (2008) Variable length LMS adaptive filter for pseudorange multipath mitigation based on SydNET stations. J Appl Geod 3(1):35–46

Pritzker Z, Feuer A (1991) Variable length stochastic gradient algorithm. IEEE Trans Signal Process 39(4):997–1001

Souza EM, Monico JFG (2004) Wavelet shrinkage: high frequency multipath reduction from GPS relative positioning. GPS Solut 8(3):152–159

Townsend B, Fenton P (1994) A practical approach to the reduction of pseudorange multipath errors in a L1 GPS receiver. In: 7th International Meeting of Satellite Division the U.S. Institute of Navigation. Salt Lake City, 20–23 Sep, pp 143–148

Townsend B, Wiebe I, Jakab A (2000) Results and analysis of using the MEDLL receiver as a multipath meter. National Technical Meeting of the U.S. Institute of Navigation, Anaheim, pp 26–29

Tranquilla JM, Carr JP, Al-Rizzo HM (1994) Analysis of a choke ring groundplane for multipath control in global positioning system applications. IEEE Trans Antennas Propag 42(7): 905–911

Van Nee RDJ (1992) The multipath estimating delay lock loop. In: IEEE 2nd International Symposium on Spread Spectrum Techniques and Applications. Yokohama, pp 39–42

Van Nee RDJ, Siereveld J, Fenton P, Townsend B (1994) The multipath estimating delay lock loop: approaching theoretical accuracy limits. In: IEEE Position, Location and Navigation Symposium. Las Vegas, pp 246–251

Walsh D (1992) Real time ambiguity resolution while on the move. In: 5th International Technical Meeting of the Satellite Division of the U.S. Institute of Navigation. Albuquerque, 16–18 Sep, pp 473–481

Weinbach U, Raziq N, Collier P (2009) Mitigation of periodic GPS multipath errors using a normalized least mean square adaptive filter. Spatial Sci 54(1):1–13

Author Biographies

Huicui Liu is a Ph.D. candidate in the School of Electronic Science and Engineering at the National University of Defense Technology, Changsha, P.R. China. She received her B.Eng. degree (2004) and M.EngSc. degree (2005) from the School of Electronic Science and Engineering at the National University of Defense Technology, specializing in satellite-based navigation. Her current research activity focuses on multipath mitigation for GNSS receivers.

Dr. Jean Xiaojing Li is an interdisciplinary researcher and currently a Research Fellow in the School of Civil and Environmental Engineering and the School of Surveying and Spatial Information Systems at the University of New South Wales (UNSW), Sydney, Australia. She obtained her Ph.D. from the School of Electrical and Telecommunications at UNSW in 2006. She is a former Japan Society for the Promotion of Science (JSPS) Postdoctoral Fellow for wind engineering researching on high-rise buildings' response to wind loads. She has been focusing on digital signal processing research for precise displacement measurement of structures with varying loading using multiple sensors such as GPS, as well as image processing and analysis on remote sensing for land observations and disaster relief.

Dr. Linlin GE is currently an Associate Professor in the School of Surveying and Spatial Information Systems at the University of New South Wales, Sydney, Australia. He obtained his B.Eng. (Hons.1) from the Wuhan Technical University of Surveying and Mapping in 1985, M.Sc. from the Institute of Seismology in 1988 and Ph.D. from the University of New South Wales in 2001. His research interests include kinematic interpretation of CORS data, structural health monitoring using GPS and other sensors, interferometer synthetic aperture radar (InSAR) and its applications, integration of remote sensing, GIS and GPS, as well as near real-time satellite remote sensing. Dr. Ge has won numerous awards for his research including the NSW Scientist of the Year 2009 award for Physics, Earth Sciences, Chemistry and Astronomy in 2009 and the Asia-Pacific Spatial Excellence Awards, the J K Barrie Award for Overall Excellence, in 2008. Further details about him can be found at: www.gmat.unsw.edu.au/LinlinGe.

Dr. Chris Rizos is a Professor and Head for the School of Surveying and Spatial Information Systems at the University of New South Wales, Sydney, Australia. He obtained both his B.Eng. (Hons.1) and Ph.D. from the University of New South Wales in 1975 and 1980, respectively. Prof Rizos has been researching the technology and applications of GPS since 1985 and has published over 400 journal and conference papers.

Dr. Feixue Wang is Full Professor and Director of the School of Electronic Science and Engineering at the National University of Defense Technology. He is responsible for research and teaching in the fields of high-precision GNSS positioning and navigation.